PHYSICAL REVIEW A **89**, 020101(R) (2014)

# Quantum-state tomography for optical polarization with arbitrary photon numbers

A. B. Klimov,[1] J. L. Romero,[1] and S. Wallentowitz[2]

[1]*Departamento de Física, Universidad de Guadalajara, Revolución 1500, 44410 Guadalajara, Jalisco, Mexico*

[2]*Instituto de Física, Pontificia Universidad Católica de Chile, Casilla 306, Santiago 22, Chile*

(Received 21 November 2013; revised manuscript received 29 January 2014; published 28 February 2014; corrected 20 March 2014)

A scheme for quantum-state tomography is presented that can be performed for polarized light with an arbitrary photon-number distribution. The proposed method fills the gap between existing polarization-tomography schemes for single-photon states and for optical fields with very large photon numbers. It consists of an optical homodyne setup triggered by the outcome of a single-photon counting module. The configuration space of polarization is parametrized by Euler angles and by an additional interference parameter, whose assessment requires conditional homodyne measurements.

DOI: 10.1103/PhysRevA.89.020101 PACS number(s): 03.65.Wj, 42.25.Ja

Optical homodyne tomography (OHT) has been very successful in the past for reconstructing the quantum state of a single-mode optical field [1]. Since its first experimental realization [2] and the development of direct reconstruction methods [3–7], the generation of several nonclassical quantum states could be proved by OHT. Among them are squeezed vacuum [8], single photons and displaced single photons [9], photonic qubits [10], photon-added coherent and thermal states [11], two-photon states [12], photon-subtracted squeezed states and squeezed Schrödinger cat states [13], and superpositions of one- and three-photon states [14]. Furthermore, the direct reconstruction methods have been complemented and partially replaced by powerful maximum-likelihood methods [15–19] that guarantee, among other properties, the physicality of the reconstructed quantum state. Alternatively, local probing of the phase space of the optical single-mode quantum state by use of unbalanced homodyning has been proposed in the past [20,21] and implemented experimentally [22].

The characterization of the quantum state of polarized light has been the subject of numerous theoretical and experimental efforts in the last years. In the case of few photons, say, one or two, the polarized light can be considered as a discrete system, so that few appropriately chosen projections allow one to determine the density matrix of the polarized light with excellent accuracy [23]. On the other hand, in the limit of very large photon numbers, a continuous-variable approach is limited in practice to the reconstruction of the so-called polarization sector [24]. The polarization sectors consist of field states with fixed photon numbers, mathematically represented by SU(2) invariant subspaces. Then the measurement of the mean Stokes vector is sufficient to reconstruct the polarization density matrix of a subspace with a fixed photon number, the latter being identified as the mean photon number of the light field. Such reconstruction schemes can be efficiently performed in experiments [25]. The quantum state in each polarization sector can be conveniently represented as an angular-momentum Wigner function [26] on a sphere [27].

However, in the intermediate case, when the number of photons is neither very small nor very large, none of the above-mentioned approaches are feasible. In this case, as in the case of very few photons, the information contained beyond the polarization sectors is crucial for the determination of the essential properties of the system. To resolve this issue, we propose here a full tomographic scheme for polarized light with arbitrary photon numbers that is based on a decomposition of the density matrix of the polarized light state in nondiagonal components on the SU(2) invariant subspaces.

Using angular-momentum notation, where the angular momentum $J=(N_{\rm H}+N_{\rm V})/2$ and its projection along the chosen quantization axis $M=(N_{\rm H}-N_{\rm V})/2$ are related to the photon numbers in the two orthogonal polarization modes $N_{\rm H}$ and $N_{\rm V}$, respectively, the complete expansion of the density operator $\hat{\varrho}$ of the two-mode field can be written as [28,29]

$$\hat{\varrho}=\sum_{J,J'=0}^{\infty}\sum_{k=|J-J'|}^{J+J'}\sum_{q=-k}^{k}\varrho_{kq}^{J'J}\hat{T}_{kq}^{J'J}, \qquad (1)$$

where the irreducible tensor operators are defined as

$$\hat{T}_{kq}^{J'J}=\sum_{M,M'}\sqrt{\frac{2k+1}{2J'+1}}C_{JM\,kq}^{J'M'}|J',M'\rangle\langle J,M|, \qquad (2)$$

with $C_{JM\,kq}^{J'M'}$ being the Clebsch-Gordan coefficients. By including nondiagonal terms $J\neq J'$, the expansion (1), together with the definition (2), is a generalization of the standard expansion within a sectorof constant $J$ (i.e., constant photon number). The off-diagonal elements $J\neq J'$ contain valid information on the coherence of the polarized light.

Substituting $J$ and $J'$ for the new variables $j=J'+J$ and $q'=J'-J$, the expansion (1) can be rewritten as

$$\hat{\varrho}=\sum_{j=0}^{\infty}\hat{\varrho}_j, \qquad (3)$$

with [30]

$$\hat{\varrho}_j=\sum_{k=\{0,\frac{1}{2}\}}^{j}\sum_{q,q'=-k}^{k}\varrho_{k\,q}^{\frac{j+q'}{2}\,\frac{j-q'}{2}}\hat{T}_{k\,q}^{\frac{j+q'}{2}\,\frac{j-q'}{2}}. \qquad (4)$$

The new parameter $j$ can be denoted as the interference parameter, as it takes account of the interference terms within the density matrix of the polarized light field. For each $j$ the interferences are between all states of different photon numbers $2J$ and $2J'$ that satisfy $J+J'=j$. The $j$ sectors of the density matrix are illustrated schematically for the simple case of a state with maximally one photon in Fig. 1.

 

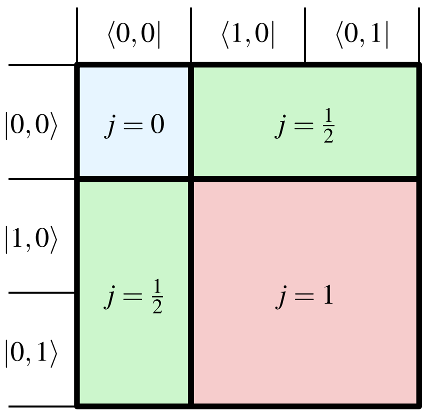


FIG. 1. (Color online) Sectors of the interference parameter $j$ in the density matrix of a state with maximally one photon [e.g., as given in Eq. (19)] with $|m,n\rangle = |m\rangle_{\rm H} \otimes |n\rangle_{\rm V}$.

As a next step, an isomorphism can be established that relates the operators $\hat{\varrho}_j$ [see Eq. (4)] to $c$-valued functions ($j$ symbols) of three Euler angles. This isomorphism is obtained from the invertible mapping [31] defined by (see Ref. [32] where the symmetrical kernel $s = 0$ has been introduced)

$$W_f^j(\Theta;s) = \mathrm{Tr}[\hat{f}\hat{\omega}_j(\Theta;s)], \tag{5}$$

$$\hat{f} = \sum_{j=0}^{\infty} \frac{j+1}{16\pi^2} \int d\Theta\, W_f^j(\Theta;-s)\hat{\omega}_j(\Theta;s), \tag{6}$$

where $W_f^j(\Theta;s)$ is the $s$-parametrized $j$ symbol of the operator $\hat{f}$, $\Theta = (\phi,\theta,\psi)$ are the three Euler angles with $\phi \in [0,2\pi]$, $\theta \in [0,\pi]$, and $\psi \in [0,4\pi]$, and $d\Theta = \sin\theta\, d\theta\, d\phi\, d\psi$. Furthermore, the rotated $s$-parametrized kernel $\hat{\omega}_j(\Theta;s)$ is defined as

$$\hat{\omega}_j(\Theta;s) = \hat{D}(\Theta)\hat{\omega}_j(0;s)\hat{D}(\Theta)^\dagger, \tag{7}$$

where $\hat{D}(\Theta) = e^{-i\phi S_z}e^{-i\theta S_y}e^{-i\psi S_z}$ is the SU(2) rotation operator [33] and the unrotated kernel reads [30]

$$\hat{\omega}_j(0;s) = \sum_{k=\{0,1/2\}}^{j} \sum_{q=-k}^{k} \left( \sqrt{\frac{j+1}{j+q+1}} C^{\frac{j+q}{2}\,\frac{j+q}{2}}_{\frac{j-q}{2}\,\frac{j-q}{2}\,kq} \right)^{-s} \times \sqrt{\frac{2k+1}{j+1}}\, \hat{T}^{\frac{j+q}{2}\,\frac{j-q}{2}}_{kq}. \tag{8}$$

Applying the mapping (5) to the density operator (3), i.e., $\hat{f} \to \hat{\rho}$, it can be seen that the kernel $\hat{\omega}_j(\Theta;s)$ chooses from the density operator $\hat{\varrho}$ only the $j$th component, i.e., $\mathrm{Tr}[\hat{\varrho}_i\hat{\omega}_j(\Theta;s)] \propto \delta_{ij}$, and that from Eq. (6) the inverse mapping is obtained as

$$\hat{\varrho}_j = \frac{j+1}{16\pi^2} \int d\Theta\, W_\varrho^j(\Theta;-s)\hat{\omega}_j(\Theta;s). \tag{9}$$

Together with Eq. (3), the relation (9) therefore allows one to reconstruct the complete density operator $\hat{\varrho}$ from its $j$ symbols $W_\varrho^j(\Theta;s)$, i.e.,

$$\hat{\rho} = \sum_j \frac{j+1}{16\pi^2} \int d\Theta\, W_\varrho^j(\Theta;-s)\hat{\omega}_j(\Theta;s). \tag{10}$$

This is the central result that facilitates an experimental reconstruction scheme by conditional balanced homodyne tomography, as will be shown later on.

The mapping (5) is a generalization of the $s$-parametrized Stratonovich-Weyl transformation [26]. That is, the standard Stratonovich-Weyl kernel [for a single $(j+1)$-dimensional irreducible representation of the SU(2) group] is obtained by integrating $\hat{\omega}_j(\Theta;s)$ over $\psi$,

$$\int_0^{4\pi} \frac{d\psi}{4\pi}\hat{\omega}_j(\Theta;s) = \sqrt{\frac{4\pi}{j+1}} \sum_{K=0}^{j} \sum_{m=-K}^{K} \left(C^{\frac{j}{2}\,\frac{j}{2}}_{\frac{j}{2}\,\frac{j}{2}\,K0}\right)^{-s} \times Y^*_{Km}(\theta,\phi)\hat{T}^{\frac{j}{2}\,\frac{j}{2}}_{Km}, \tag{11}$$

where only integer values of the interference parameter $j$ appear [$\int_0^{4\pi} d\psi\hat{\omega}_j(\Theta;s) = 0$ for semi-integer $j$]. As only diagonal elements of the irreducible tensor operator with respect to the photon number (here proportional to $j$) are taken into account, such a representation corresponds to the well-known polarization sectors with fixed photon numbers [34]. The main advantage of the mapping (10) consists in preserving the full information about the complete density operator and not only of its components stored in SU(2) irreducible subspaces.

To proceed, $s = -1$ is chosen in Eq. (10), from which one obtains

$$\hat{\varrho} = \sum_j \frac{j+1}{16\pi^2} \int d\Theta \langle\hat{Q}_j(\Theta)\rangle \hat{P}_j(\Theta), \tag{12}$$

where the kernel of the P function is $\hat{P}_j(\Theta) = \hat{\omega}_j(\Theta; s=1)$. The expectation value of the kernel of the Q function, $\hat{Q}_j(\Theta) = \hat{\omega}_j(\Theta;s=-1)$, can be rewritten as $\langle\hat{Q}_j(\Theta)\rangle = \mathrm{Tr}[\hat{\varrho}\hat{Q}_j(\Theta)] = \mathrm{Tr}[\hat{\varrho}(\Theta)\hat{Q}_j(0)]$, where $\hat{Q}_j(0) = \hat{\omega}_j(0;s=-1)$ is the unrotated kernel, and the rotated quantum state reads

$$\hat{\varrho}(\Theta) = \hat{D}^\dagger(\Theta)\hat{\varrho}\hat{D}(\Theta). \tag{13}$$

The unrotated kernel of the Q function can be shown to reduce to the simple form [30,35]

$$\hat{Q}_j(0) = \sum_{q=-j}^{j} \left|\frac{j+q}{2},\frac{j+q}{2}\right\rangle\left\langle\frac{j-q}{2},\frac{j-q}{2}\right|. \tag{14}$$

Rewriting the above expression in terms of the photon-number states in the two polarization modes with photon numbers $N_{\rm H,V} = J \pm M$, it is readily seen that the polarization modes are factorized with one of the modes being in the vacuum state:

$$\hat{Q}_j(0) = \sum_{q=-j}^{j} |j+q\rangle_{\rm HH}\langle j-q| \otimes |0\rangle_{\rm VV}\langle 0|. \tag{15}$$

The appearance of the factorized vacuum state in the V mode is due to the choice of the quantization axis of the angular momentum state, i.e., due to the definition $M = (N_{\rm H} - N_{\rm V})/2$: The unrotated kernel, by definition, corresponds to the north pole of the Poincaré sphere ($\theta = \phi = \psi = 0$), where $M = J$ and thus necessarily $N_{\rm V} = 0$.

Furthermore, also the kernel of the P function can be explicitly written in terms of the photon-number states as [30]

$$\hat{P}_j(\Theta) = \sum_{k=\{0,1/2\}}^{j} \sum_{q,q'=-k}^{k} D^k_{qq'}(\Theta) \sum_{m=-\frac{j-q'}{2}}^{\frac{j-q'}{2}} \sum_{m'=-\frac{j+q'}{2}}^{\frac{j+q'}{2}} C^{\frac{j+q'}{2}m'}_{\frac{j-q'}{2}m\,kq}$$
$$\times \frac{2k+1}{j+1}\sqrt{\frac{(j+k+1)!(j-k)!}{(j+q'+1)!(j-q')!}}$$
$$\times \left|\frac{j+q'}{2}+m'\right\rangle_{\rm HH}\left\langle\frac{j-q'}{2}+m\right|$$
$$\otimes \left|\frac{j+q'}{2}-m'\right\rangle_{\rm VV}\left\langle\frac{j-q'}{2}-m\right|. \qquad (16)$$

Thus to implement an experimental scheme for obtaining the complete information on the quantum state of the polarized light field, the input optical field has to be unitarily transformed according to (13) and then the expectation value of (15) should be measured for the transformed field. Whereas the transformation (13) corresponds to a rotation of the three Euler angles of the polarization of the input field, which can be implemented in experiments by a combination of wave plates, the required expectation value can be obtained from conditional balanced homodyne tomography: The expectation value (15) can be rewritten as

$$\langle\hat{Q}_j(\Theta)\rangle = \int dx \int d\varphi S_j(x,\varphi)p_\Theta(x;\varphi|N_{\rm V}=0), \qquad (17)$$

where $p_\Theta(x;\varphi|N_{\rm V}=0)$ is the probability density for the quadrature value $x$ at phase $\varphi$ in mode H, conditioned on $N_{\rm V}=0$ photons being present in mode V, for the input field being rotated in polarization by the Euler angles $\Theta$. The sampling functions are obtained as

$$S_j(x,\varphi) = \sum_{m=-j}^{j} f_{j-m,j+m}(x)e^{-2im\varphi}, \qquad (18)$$

where the tomographic pattern functions $f_{m,n}(x) = \frac{\partial}{\partial x}[\Phi_{{\rm reg},m}(x)\Phi_{{\rm irreg},n}(x)]$, with $\Phi_{{\rm reg},n}(x)$ and $\Phi_{{\rm irreg},n}(x)$ being the $n$th regular and irregular eigenfunctions of the harmonic oscillator, respectively, that can by obtained from recurrence relations [6,7].

Therefore, the required data for the reconstruction of the complete quantum state of an arbitrary two-mode polarized light field can be obtained from a conditional balanced-homodyne tomographic setup, as shown in Fig. 2. The input field is rotated in polarization by the wave plates that fix the angles $\theta$, $\phi$, and $\psi$. Then two orthogonal polarizations are separated by the polarizing beam splitter (PBS) and the vertical mode is measured with a single-photon counting module (SPCM). Conditioned on a no-count event in mode V, the phase-dependent quadrature statistics of the horizontal mode is obtained in the balanced-homodyne setup, comprising the beam splitter BS, the two high-efficiency photodetectors PD1 and PD2, and the local oscillator LO with corresponding phase control.

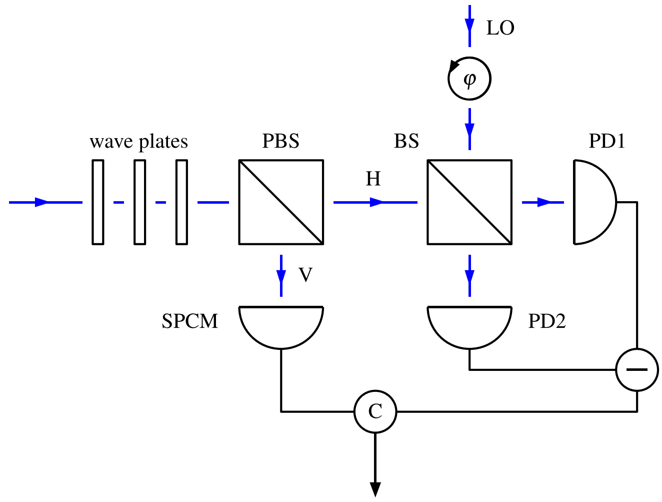


FIG. 2. (Color online) Conditional balanced homodyne measurement: The wave plates realize the rotation by the angles $\Theta$, and the polarizing beam splitter (PBS) separates the V and H modes, where the V mode is detected by a single-photon counting module (SPCM). Conditioned on a no-count event in the V mode, the H mode is measured in the balanced homodyne scheme with a beam splitter (BS), phase-controlled local oscillator (LO), and two photodetectors (PD1, PD2).

Since the interference parameter $j$ does not describe subspaces with a definite photon number, it may not be very intuitive to see how the angle-dependent expectation values $\langle\hat{Q}_j(\Theta)\rangle$ appear for a given quantum state $\hat{\varrho}$. The visualization of $\langle\hat{Q}_j(\Theta)\rangle$ is not that transparent as for the case of the standard angular momentum functions $Q^J_\rho(\theta,\phi)$ that represent states with a fixed value of $J$ (i.e., photon number).

For instance, the single-photon state with a vacuum contribution,

$$|\Psi_1\rangle = \left[|0\rangle_{\rm H}\otimes|0\rangle_{\rm V} + (|1\rangle_{\rm H}\otimes|0\rangle_{\rm V} + |0\rangle_{\rm H}\otimes|1\rangle_{\rm V})\,e^{i\frac{\psi_0}{2}}\right]\big/\sqrt{3}, \qquad (19)$$

requires the expectation values with an interference parameter $j = 0,\frac{1}{2},1$ for its complete description:

$$\langle\hat{Q}_0(\Theta)\rangle_1 = \frac{1}{3}, \qquad (20)$$

$$\langle\hat{Q}_{\frac{1}{2}}(\Theta)\rangle_1 = \frac{2}{3}\left[\cos\frac{\theta}{2}\cos\left(\frac{\phi+\psi+\psi_0}{2}\right) + \sin\frac{\theta}{2}\cos\left(\frac{\phi-\psi-\psi_0}{2}\right)\right], \qquad (21)$$

$$\langle\hat{Q}_1(\Theta)\rangle_1 = \frac{1}{3}(1+\sin\theta\cos\phi). \qquad (22)$$

The phase-space description (20)–(22) of the state (19) is shown in Fig. 3. Returning to Fig. 1, an interpretation of the interference parameter $j$ can be obtained as follows: The $j=0$ phase-space distribution is perfectly isotropic (see the upper plot in Fig. 3) as it corresponds to the admixture of the vacuum state (see Fig. 1). On the other hand, the $j=\frac{1}{2}$

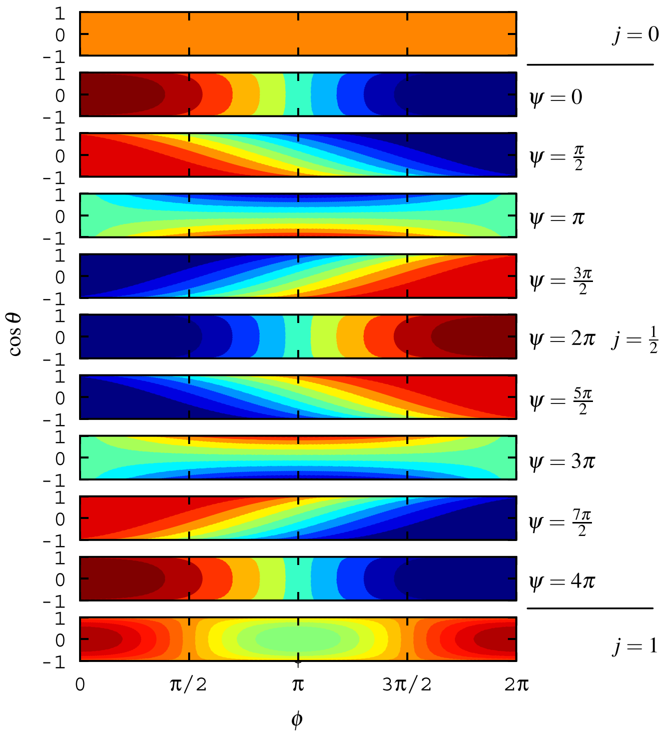


FIG. 3. (Color online) Phase-space image of a single-photon state with a vacuum contribution, according to Eq. (19) with $\psi_0 = 0$. Dark red and dark blue correspond to the maximum positive value $+\frac{2}{3}$ and minimum negative value $-\frac{2}{3}$, respectively, of the phase-space distributions $\langle \hat{Q}_j(\Theta)\rangle$.

distribution depends on all three Euler angles (see the middle plots in Fig. 3). This phase-space distribution corresponds to the interference terms where exactly one photon participates, i.e., the interference between single-photon and vacuum states (see Fig. 1). Finally, the $j = 1$ distribution depends only on the first two Euler angles (see the lower plot in Fig. 3), and corresponds to interference with the participation of two photons, i.e., between single-photon states of both polarization modes (see Fig. 1). Thus, the interference parameter $j$ groups all the interference terms in the density matrix that correspond to a participation of $2j$ photons.

Another example for the phase-space description of a polarized light field is that of a two-mode coherent state $|\Psi_{\rm cs}\rangle = |\alpha\rangle_{\rm H} \otimes |\beta\rangle_{\rm V}$. In this case one has

$$\langle \hat{Q}_j(\Theta)\rangle_{\rm cs} = e^{-r^2}\left(\frac{r\cos\theta'}{2}\right)^{2j} \sum_{q=-j}^{j} \frac{e^{2iq(\phi'+\psi')}}{\sqrt{(j+q)!(j-q)!}}, \tag{23}$$

where the angles $\Theta' = (\phi',\theta',\psi')$ are obtained as a composition of the Euler angles $\Theta_0$ defined by

$$\alpha = \frac{r\cos\theta_0}{2} e^{-i(\varphi_0+\psi_0)/2}, \tag{24}$$

$$\beta = \frac{r\sin\theta_0}{2} e^{-i(\psi_0-\varphi_0)/2}, \tag{25}$$

and $\Theta$ in the standard way [36]. For a large average total photon number, Eq. (23) simplifies to

$$\langle \hat{Q}_j(\Theta)\rangle_{\rm cs} = \sqrt{2\pi j}\,\frac{(r\cos\theta')^{2j}}{j!} e^{-r^2-2j\sin^2(\phi'+\psi')} \tag{26}$$

for the integer and

$$\langle \hat{Q}_j(\Theta)\rangle_{\rm cs} = \sqrt{2\pi}\,\frac{(r\cos\theta')^{2j}}{\left(j-\frac{1}{2}\right)!} \cos(\phi'+\psi') e^{-r^2-2j\sin^2(\phi'+\psi')} \tag{27}$$

for semi-integer values of the interference parameter $j$, correspondingly.

Finally, the two-mode thermal state,

$$\hat{\varrho}_{\rm th} = \frac{1}{(1+\bar{N})^2}\left(\frac{\bar{N}}{1+\bar{N}}\right)^{\hat{N}_{\rm H}+\hat{N}_{\rm V}}, \tag{28}$$

corresponds to the isotropic distribution ($j = 0,1,2,\ldots$)

$$\langle \hat{Q}_j(\Theta)\rangle_{\rm th} = \frac{1}{(1+\bar{N})^2}\left(\frac{\bar{N}}{1+\bar{N}}\right)^{j}. \tag{29}$$

In summary, we have presented a scheme that allows one to achieve a complete tomographic reconstruction of the optical polarization quantum state. In contrast to the standard polarization tomography scheme [24,25] that may reconstruct the quantum state only in subspaces with fixed photon numbers (polarization sectors), the proposed scheme surpasses this limitation by the use of conditional homodyne measurements. These measurements are conditioned on no detection of photons in one of the polarization modes that has to be performed on the single-photon level. Such a setup is required in order to reconstruct the complete density matrix of the polarization quantum state. Our method is based on the isomorphism (5), which generalizes the conventional mapping onto the polarization sectors.

Experimental setups similar to that proposed here have been realized successfully in the past, e.g., for quantum-state tomography of single photons [1,9]. In these experiments, heralded single photons were tomographically reconstructed, which requires the registration of events with nonzero photon numbers at a SPCM. In the scheme presented here, events with zero photon counts need to be registered. Therefore, to ensure the true absence of a V photon for each no-count event, a SPCM with very high quantum efficiency must be employed. Under such circumstances our proposal would be experimentally feasible and it would provide deeper insight into the polarization properties of light fields with arbitrary photon numbers, in particular, for intermediate photon numbers, i.e., for more than one photon but still far from the semiclassical limit.

This research was supported by CONICYT, DRI "Programa de Cooperación Científica Internacional" CONICYT/CONACYT 2011557, and CONACYT 174713.

[1] A. I. Lvovsky and M. G. Raymer, Rev. Mod. Phys. **81**, 299 (2009).
[2] D. T. Smithey, M. Beck, M. G. Raymer, and A. Faridani, Phys. Rev. Lett. **70**, 1244 (1993); D. T. Smithey, M. Beck, J. Cooper, and M. G. Raymer, Phys. Rev. A **48**, 3159 (1993); D. T. Smithey, M. Beck, J. Cooper, and A. Faridani, Phys. Scr. T **48**, 35 (1993).
[3] K. Vogel and H. Risken, Phys. Rev. A **40**, 2847 (1989).
[4] G. M. D'Ariano, C. Macchiavello, and M. G. A. Paris, Phys. Rev. A **50**, 4298 (1994).
[5] G. M. D'Ariano, M. G. A. Paris, and M. F. Sacchi, in *Quantum State Estimation*, edited by M. G. A. Paris and J. Rehacek, Lecture Notes in Physics Vol. 649 (Springer, Berlin, 2004), p. 7.
[6] T. Richter, Phys. Lett. **211**, 327 (1996).
[7] U. Leonhardt *et al.*, Opt. Commun. **127**, 144 (1996).
[8] M. Vasilyev, S. K. Choi, P. Kumar, and G. Mauro D'Ariano, Phys. Rev. Lett. **84**, 2354 (2000); J. Wenger *et al.*, Eur. Phys. J. D **32**, 391 (2005); V. D'Auria *et al.*, Phys. Rev. Lett. **102**, 020502 (2009).
[9] A. I. Lvovsky *et al.*, Phys. Rev. Lett. **87**, 050402 (2001); A. I. Lvovsky and S. A. Babichev, Phys. Rev. A **66**, 011801(R) (2002); A. Zavatta, S. Viciani, and M. Bellini, Science **306**, 660 (2004); J. S. Neergaard-Nielsen *et al.*, Opt. Express **15**, 7940 (2007).
[10] A. I. Lvovsky and J. Mlynek, Phys. Rev. Lett. **88**, 250401 (2002); S. A. Babichev, J. Ries, and A. I. Lvovsky, Europhys. Lett. **64**, 1 (2003); S. A. Babichev, B. Brezger, and A. I. Lvovsky, Phys. Rev. Lett. **92**, 047903 (2004); S. A. Babichev, J. Appel, and A. I. Lvovsky, *ibid.* **92**, 193601 (2004); A. Zavatta, M. D'Angelo, V. Parigi, and M. Bellini, *ibid.* **96**, 020502 (2006); M. D'Angelo, A. Zavatta, V. Parigi, and M. Bellini, Phys. Rev. A **74**, 052114 (2006).
[11] A. Zavatta, S. Viciani, and M. Bellini, Phys. Rev. A **70**, 053821 (2004); **72**, 023820 (2005); A. Zavatta, V. Parigi, and M. Bellini, *ibid.* **75**, 052106 (2007); V. Parigi *et al.*, Science **317**, 1890 (2007).
[12] A. Ourjoumtsev, R. Tualle-Brouri, and P. Grangier, Phys. Rev. Lett. **96**, 213601 (2006).
[13] J. Wenger, R. Tualle-Brouri, and P. Grangier, Opt. Lett. **29**, 1267 (2004); J. S. Neergaard-Nielsen, B. M. Nielsen, C. Hettich, K. Molmer, and E. S. Polzik, Phys. Rev. Lett. **97**, 083604 (2006); A. Ourjoumtsev *et al.*, Nature (London) **448**, 784 (2007).
[14] A. Ourjoumtsev *et al.*, Science **312**, 83 (2006); K. Wakui *et al.*, Opt. Express **15**, 3568 (2007).
[15] K. Banaszek, Phys. Rev. A **57**, 5013 (1998); Acta Phys. Slovaca **48**, 185 (1998); Phys. Rev. A **59**, 4797 (1999); K. Banaszek, G. M. D'Ariano, M. G. A. Paris, and M. F. Sacchi, *ibid.* **61**, 010304(R) (1999).
[16] J. Rehacek, Z. Hradil, and M. Jezek, Phys. Rev. A **63**, 040303(R) (2001).
[17] Z. Hradil *et al.*, in *Quantum State Estimation* (Ref. [5]), p. 59.
[18] A. I. Lvovsky, J. Opt. B **6**, S556 (2004).
[19] Z. Hradil, D. Mogilevtsev, and J. Rehacek, Phys. Rev. Lett. **96**, 230401 (2006); D. Mogilevtsev, J. Rehacek, and Z. Hradil, Phys. Rev. A **75**, 012112 (2007); J. Rehacek, Z. Hradil, E. Knill, and A. I. Lvovsky, *ibid.* **75**, 042108 (2007).
[20] S. Wallentowitz and W. Vogel, Phys. Rev. A **53**, 4528 (1996); K. Banaszek and K. Wodkiewicz, Phys. Rev. Lett. **76**, 4344 (1996); T. Opatrny *et al.*, J. Mod. Opt. **44**, 2405 (1997).
[21] Z. Kis *et al.*, Phys. Rev. A **59**, R39 (1999); S. Wallentowitz, B. Seifert, and S. Godoy, New J. Phys. **14**, 105019 (2012).
[22] K. Banaszek, C. Radzewicz, K. Wodkiewicz, and J. S. Krasinski, Phys. Rev. A **60**, 674 (1999); A. Allevi *et al.*, *ibid.* **80**, 022114 (2009); M. Bondani, A. Allevi, and A. Andreoni, Opt. Lett. **34**, 1444 (2009); K. Laiho, K. N. Cassemiro, D. Gross, and C. Silberhorn, Phys. Rev. Lett. **105**, 253603 (2010).
[23] R. B. A. Adamson and A. M. Steinberg, Phys. Rev. Lett. **105**, 030406 (2010); L. Sansoni *et al.*, *ibid.* **105**, 200503 (2010); J. B. Altepeter *et al.*, Opt. Express **19**, 26011 (2011).
[24] V. P. Karassiov, J. Phys. A: Math. Gen. **26**, 4345 (1993); V. P. Karassiov and A. V. Masalov, J. Exp. Theor. Phys. **99**, 51 (2004).
[25] M. G. Raymer and A. C. Funk, Phys. Rev. A **61**, 015801 (1999); C. Marquardt *et al.*, Phys. Rev. Lett. **99**, 220401 (2007); C. R. Müller *et al.*, New J. Phys. **14**, 085002 (2012).
[26] R. L. Stratonovich, Sov. Phys. JETP **4**, 891 (1957) [J. Exp. Theor. Phys. **31**, 1012 (1956)]; G. S. Agarwal, Phys. Rev. A **24**, 2889 (1981); C. Brif and A. Mann, J. Phys. A: Math. Gen. **31**, L9 (1998); J. C. Varilly and J. M. Gracia-Bondia, Ann. Phys. **190**, 107 (1989).
[27] J. P. Dowling, G. S. Agarwal, and W. P. Schleich, Phys. Rev. A **49**, 4101 (1994).
[28] U. Fano, Rev. Mod. Phys. **29**, 74 (1957).
[29] Here the $J$ and $J'$ sums run over integer and semi-integer values.
[30] Here the $k$ and $q^{(\prime)}$ sums run over integer or semi-integer values according to the value of $j$.
[31] This mapping satisfies all the Stratonovich-Weyl conditions, i.e., hermiticity, covariance under SU(2) transformations, and normalization [26].
[32] A. B. Klimov and J. L. Romero, J. Phys. A: Math. Theor. **41**, 055303 (2008).
[33] The matrix elements of this rotation operator define the Wigner $D$ function in the Euler parametrization $D^{J}_{mm'}(\Theta) = \langle J,m|\hat{D}(\Theta)|J,m'\rangle$.
[34] In particular, for $s=-1$, $\int_0^{4\pi}\frac{d\psi}{4\pi}\hat{\omega}_j(\Theta;s=-1) = |\frac{j}{2};\phi,\theta\rangle\langle\frac{j}{2};\phi,\theta|$, with $|\frac{j}{2};\phi,\theta\rangle$ being standard SU(2) coherent states with angular momentum $j/2$.
[35] See Supplemental Material at http://link.aps.org/supplemental/10.1103/PhysRevA.89.020101 for the derivation of this result.
[36] D. A. Varshalovich, A. N. Moskalev, and V. K. Khersonskiĭ, *Quantum Theory of Angular Momentum* (World Scientific, Singapore, 1988).